Intracellular hydroxyproline imprinting following resolution of bleomycin-induced pulmonary fibrosis

Shengren Song[1,2,3,6], Zhenli Fu[2,6], Ruijuan Guan[4,6], Jie Zhao[5,6], Penghui Yang[2,6], Yang Li[5], Hang Yin[2], Yunxin Lai[2], Gencheng Gong[2], Simin Zhao[2], Jiangtian Yu[4], Xiaomin Peng[2], Ying He[2], Yumei Luo[2], Nanshan Zhong[1,2,7] and Jin Su[2,4,7]

[1]Dept of Pathophysiology, Guizhou Medical University, Guiyang, China. [2]State Key Laboratory of Respiratory Diseases, National Clinical Research Center for Respiratory Diseases, Guangzhou Institute of Respiratory Health, First Affiliated Hospital of Guangzhou Medical University, Guangzhou, China. [3]Affiliated Hospital of Guizhou Medical University, Guiyang, China. [4]Shenzhen International Institute for Biomedical Research, Shenzhen, China. [5]Guangdong Provincial Key Laboratory of Biomedical Imaging and Guangdong Provincial Engineering Research Center of Molecular Imaging, The Fifth Affiliated Hospital, Sun Yat-sen University, Zhuhai, China. [6]Shengren Song, Zhenli Fu, Ruijuan Guan, Jie Zhao and Penghui Yang contributed equally to this work. [7]Jin Su and Nanshan Zhong contributed equally as lead authors and supervised the work.

Corresponding author: Jin Su (sujin@gird.cn)

Shareable abstract (@ERSpublications)
The self-resolving nature of the best-accepted model for lung fibrosis is well reflected by several improved methods but fails to be monitored by classical hydroxyproline assay, emphasising the need to use assessment methods suited to the disease window https://bit.ly/3AsJzSL

Cite this article as: Song S, Fu Z, Guan R, *et al*. Intracellular hydroxyproline imprinting following resolution of bleomycin-induced pulmonary fibrosis. *Eur Respir J* 2022; 59: 2100864 [DOI: 10.1183/13993003.00864-2021].

Received: 23 March 2021
Accepted: 14 Sept 2021

Abstract

Background Idiopathic pulmonary fibrosis (IPF) is a fatal lung disease with few treatment options. The poor success in developing anti-IPF strategies has impelled researchers to reconsider the importance of the choice of animal model and assessment methodologies. Currently, it is still not settled whether the bleomycin-induced lung fibrosis mouse model finally returns to resolution.

Methods This study aimed to follow the dynamic fibrotic features of bleomycin-treated mouse lungs over extended durations through a combination of the latest technologies (micro-computed tomography imaging and histological detection of degraded collagens) and traditional methods. In addition, we also applied immunohistochemistry to explore the distribution of all hydroxyproline-containing molecules.

Results As determined by classical biochemical methods, total lung hydroxyproline contents reached a peak at 4 weeks after bleomycin injury and maintained a steady high level thereafter until the end of the experiments (16 weeks). This result seemed to partially contradict with the changes of other fibrosis evaluation parameters, which indicated a gradual degradation of collagens and a recovery of lung aeration after the fibrosis peak. This inconsistency was well reconciled by our data from immunostaining against hydroxyproline and fluorescent peptide staining against degraded collagen, together showing large amounts of hydroxyproline-rich degraded collagen fragments detained and enriched within the intracellular regions at 10 or 16 weeks rather than at 4 weeks after bleomycin treatment.

Conclusions Our present data not only offer respiratory researchers a new perspective towards the resolution nature of mouse lung fibrosis, but also remind them to be cautious when using the hydroxyproline content assay to evaluate the severity of fibrosis.

Introduction

Idiopathic pulmonary fibrosis (IPF), characterised by distortion of the lung architecture and deposition of extracellular matrix (ECM), is a chronic, progressive and usually lethal lung disease of unknown aetiology, with a 5-year survival of ∼20% [1]. IPF affects ∼5 million people worldwide and its incidence increases dramatically with age [2]. According to data from a recent review by Kolb *et al.* [3], there were a total of 145 IPF clinical trials published between 2008 and 2019 that investigated 93 compounds/combinations. Disappointingly, these tremendous investments only facilitated the approval of two drugs (pirfenidone and

nintedanib). Albeit having shown some benefits in slowing down the pace of lung function decline, these two anti-fibrotic drugs failed to improve overall survival of IPF patients [4].

Experimental models are indispensable and crucial tools for understanding the pathogenesis of lung diseases as well as for evaluating drug efficacy prior to conducting clinical trials. The poor success in developing anti-IPF strategies has impelled many researchers and experts to reinforce and emphasise the importance of the choice of the appropriate animal model and reliable assessment methodologies in recent years [3, 5–9]. Intratracheal instillation of bleomycin in mice, albeit having limitations, is still the most frequently used and best-accepted lung fibrosis model due to its gross similarities to IPF patients, low cost, relative ease of induction and high reproducibility [6, 9]. There is, at least, one consensus about this model: inflammatory infiltration usually occurs within 7 days, followed by a gradual accumulation of ECM proteins thereafter and a peak fibrotic response at ∼3–4 weeks later [3]. However, one point still remaining unsettled is whether bleomycin-induced fibrotic lung injury finally returns to normal or partial resolution [9]. Early studies claimed to observe a self-limiting response of fibrosis in mice [10–13], which contrasts with the progressive and irreversible nature of human IPF. On the contrary, there are other reports showing that bleomycin-induced fibrosis in C57BL/6J mice can persist for up to 3–6 months and the injury in the lung never resolves [14, 15]. The reason for this discrepancy remains unresolved and was speculated to be associated with the dosing of bleomycin and/or the murine strains used by different researchers [9].

Considering that the readouts for fibrosis intensity and distribution adopted by previous studies were mostly achieved through sacrificing animals at various time-points, it is necessary to combine noninvasive approaches with optimised classical methods so as to reconcile the debate. Conventional methodologies used for lung fibrosis assessments include biochemical quantification of collagen (hydroxyproline content as a surrogate or Sirius red staining), histological assessment of fibrotic distribution (Masson's trichrome staining) and gene expression analysis of fibrotic markers. Due to the patchy distribution of bleomycin-induced fibrotic lesions as well as the inherent bias associated with morphological scoring systems, the 2017 American Thoracic Society guidelines strongly recommended hydroxyproline measurement of whole-lung homogenates as the optimal primary end-point for pre-clinical assessment of potential therapies against pulmonary fibrosis [6], while gene expression studies were suggested to be used accompanied with biochemical parameters. To decrease the observer-dependent variability of morphological examination and scoring systems, advanced computer machine learning tools were recently developed and utilised to quantitatively analyse the fibrotic areas on whole-slide images of lung tissues from either animal models or human patients [16, 17].

Computed tomography (CT), a noninvasive imaging technique that provides accurate longitudinal information, now plays a central role in the diagnosis of IPF *via* recognition of usual interstitial pneumonia patterns characterised by reticulation and honeycomb cysts of subpleural and bibasilar distribution [18]. Because this clinically relevant method complies with "the 3R rules" (Refinement, Replacement, Reduction) in animal experimentation, micro-CT has commonly been applied to small rodent pulmonary fibrosis models [15, 19–21]. Representative two-dimensional micro-CT images of the lung were initially used to depict the severity of lung injury in animals. Due to the patchy and heterogeneous nature of the bleomycin-induced model, it later became a tendency to perform three-dimensional reconstruction of the lung CT images in order to measure the residual lung volumes according to the corresponding range of Hounsfield Unit values, a quantitative radiodensity scale [22–24]. Notably, by selecting pixels with a Hounsfield Unit range from −121 to 121 HU, lung CT images of the bleomycin mouse model were subtly segmented into four zones with different aeration status, including normal aeration, poor aeration, hyperinflation as well as nonaeration [23].

Here, we aimed to dynamically follow the fibrotic features of bleomycin-treated mouse lungs over extended durations (up to 16 weeks) through a combination of the aforementioned latest technologies and traditional methods.

Methods

For detailed methods, including animal protocols and experimental procedures, see the supplementary material.

Ethics statement

All animal experiments were approved by the Animal Care and Use Committee of Guangzhou Medical University (Guangzhou, China), and were performed in strict accordance with approved guidelines.

Statistics

Data were processed with Prism version 6.0 (GraphPad, San Diego, CA, USA) and are expressed as mean±SEM. One-way ANOVA with the Bonferroni *post hoc* test was used to compare differences among various groups. $p<0.05$ was considered statistically significant.

Results

Biochemical determination of collagen content

In order to dynamically characterise the fibrosis patterns in bleomycin-treated lungs, mice receiving a single intratracheal instillation of bleomycin were sacrificed at various intervals for up to 16 weeks after injury (figure 1a). The whole-lung tissue homogenates were first subjected to a colorimetric-based hydroxyproline assay, a highly recommended method for collagen content determination [6, 25, 26]. The results showed that total lung hydroxyproline levels were inclined to gradually increase from week 1 to week 4 and were maintained unchanged thereafter (figure 1b). Because some of the aforementioned

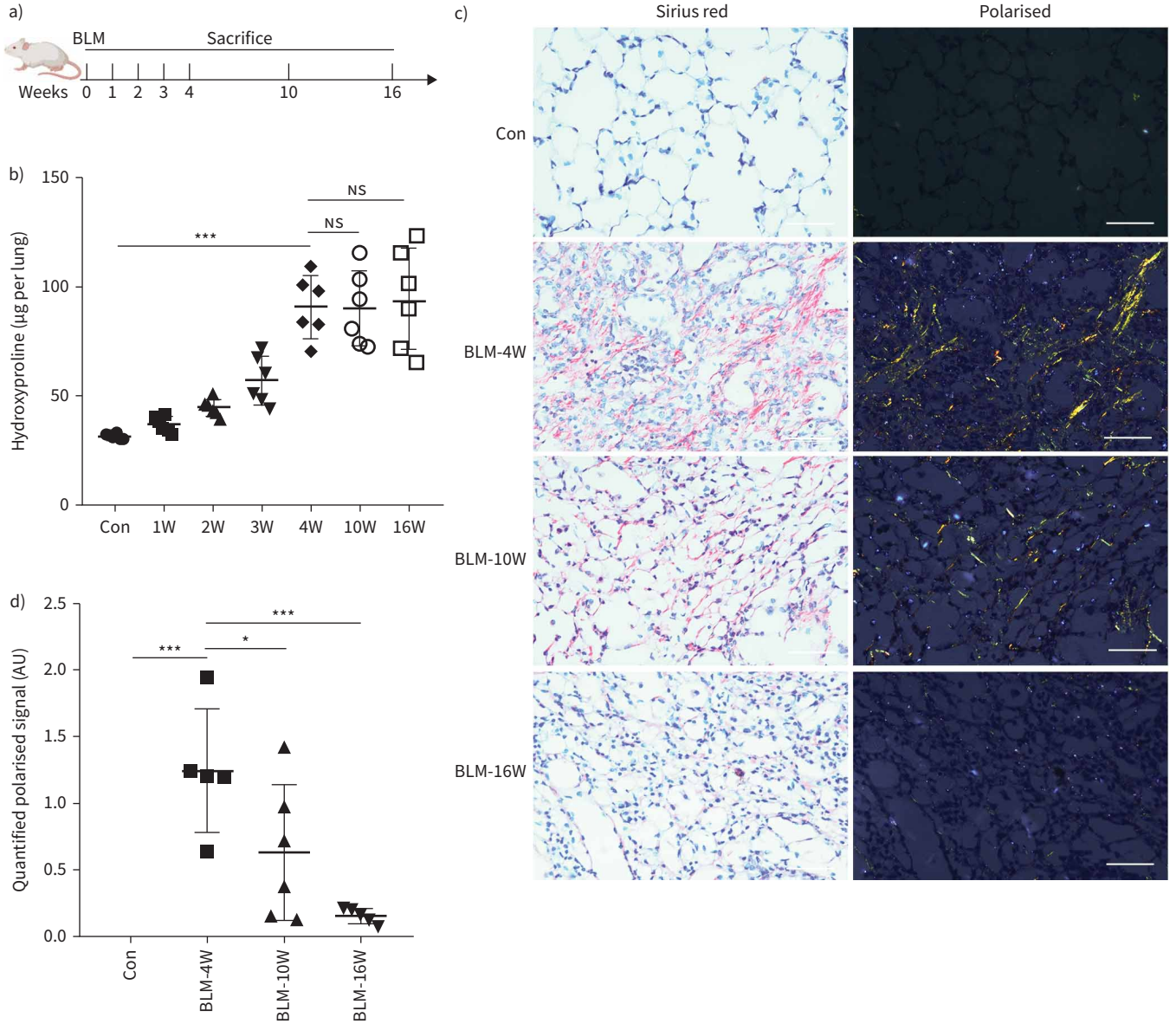

FIGURE 1 Lung collagen measurement by biochemical methods during the process of experimental lung fibrosis. a) The scheme of mice sacrifice following bleomycin (BLM) instillation. b) Colorimetric-based hydroxyproline assay of bleomycin- or saline-treated mice. c) Sirius red staining of lung tissue sections. The collagen fibres were visualised by polarised light microscopy. Scale bar: 100 µm. d) Quantification of polarised light signals (arbitrary units (AU)) by Image J. Data are expressed as mean±SD, n=6. *: $p<0.05$; ***: $p<0.001$; NS: nonsignificant. Con: control; W: weeks.

observed phenomena were apparently contradictory with the data reported elsewhere showing that the bleomycin-induced lung hydroxyproline content usually dropped to the basal level from 8 weeks onwards [12, 27, 28], another batch of mice was utilised to repeat this study. It was demonstrated that from week 4 to week 16, mouse hydroxyproline levels remained steadily high (supplementary figure), implying that the data from our model system were highly repeatable and confirmed.

To further test whether the lung hydroxyproline contents in the bleomycin-induced mouse model were in proportion to their corresponding amounts of native collagens, Sirius red staining that allows analysis of "newly formed" collagen fibres was then performed on the same animals. Unlike the alteration patterns in hydroxyproline, collagen fibres displayed a dramatic increase at 4 weeks but significantly trended downwards at 16 weeks of follow-up (figure 1c and d). These results indicate that the fibrotic lung micro-environment in mice might shift from collagen synthesis to degradation following week 4.

Gene expression analysis of ECM molecules

Gene expression analysis of major components of the ECM represents another option for the assessment of the severity of lung fibrosis [6]. As demonstrated by the results of real-time quantitative PCR (qPCR) and Western blotting (figure 2a–c and supplementary figure), mRNA and protein expression of both fibronectin and collagen I were markedly elevated to peak values at around week 2–3, followed by a reduction to the basal level at week 16, suggesting that the deposited ECM induced by bleomycin in mice might have reached to a peak prior to week 4.

Quantification of the extent of lung damage as well as collagen structure on histological images

Next, the structural changes of the bleomycin-treated lung were histopathologically examined by haematoxylin/eosin staining. To minimise observer-dependent biases, stained lung tissue sections were

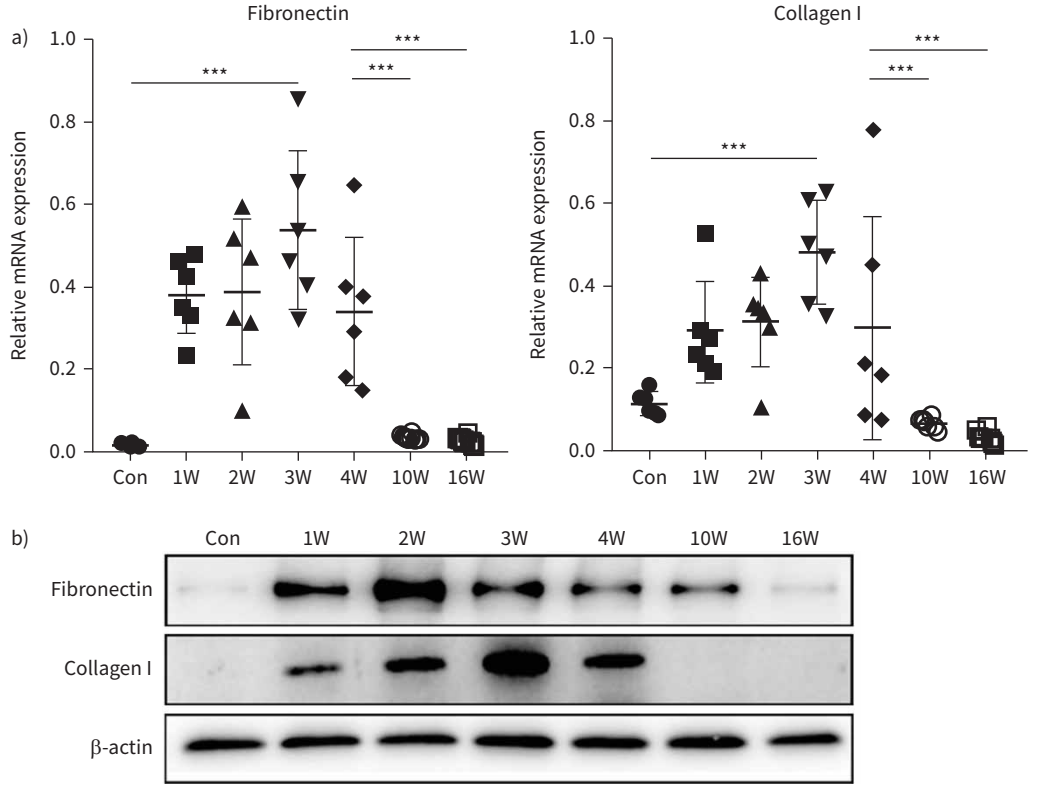

FIGURE 2 Gene expression of extracellular matrix markers. Mouse lung tissues at the indicated time-points were subjected to a) either real-time quantitative PCR (qPCR) or b) immunoblot analysis of the expression levels of collagen I and fibronectin. Glyceraldehyde 3-phosphate dehydrogenase and β-actin were used as internal reference controls for qPCR and immunoblotting, respectively. Data are expressed as mean±SD, n=6. ***: p<0.001. Con: control; W: weeks.

scanned by a commercial whole-slide image scanner to obtain high-resolution digital images of entire sections and then subjected to quantitative calculation of damaged areas by use of a novel automated tool called Orbit Image Analysis [16]. Consistent with the collagen expression data, the proportions of injured regions exhibited a significant augmentation from week 1 to week 4 and then appeared to decrease from week 10 to week 16 (figure 3a and b).

The hallmark structure of collagen is the triple helix where three linear protein chains assemble into a trimeric form. Upon being fragmented by proteases such as the matrix metalloproteinases, the collagen molecule denatures as the triple helix unfolds [29]. Collagen hybridisation peptide (CHP) is a synthetic peptide that can specifically bind to such degraded and denatured collagen molecules, but not to intact collagen [29]. Using fluorescently labelled CHP (Cy5-CHP), we tested whether the molecular structure of collagen in the lung tissue is intact at week 16. There were minimal fluorescent CHP signals in the interstitial areas in normal lung and the signal gradually increased from week 1 to week 4 of fibrosis (figure 4a and b). The fluorescence intensity peaked at week 16, at a level that was significantly higher than week 4. These data strongly support the concept that the collagen matrix did undergo a degradative process from week 4 to week 16.

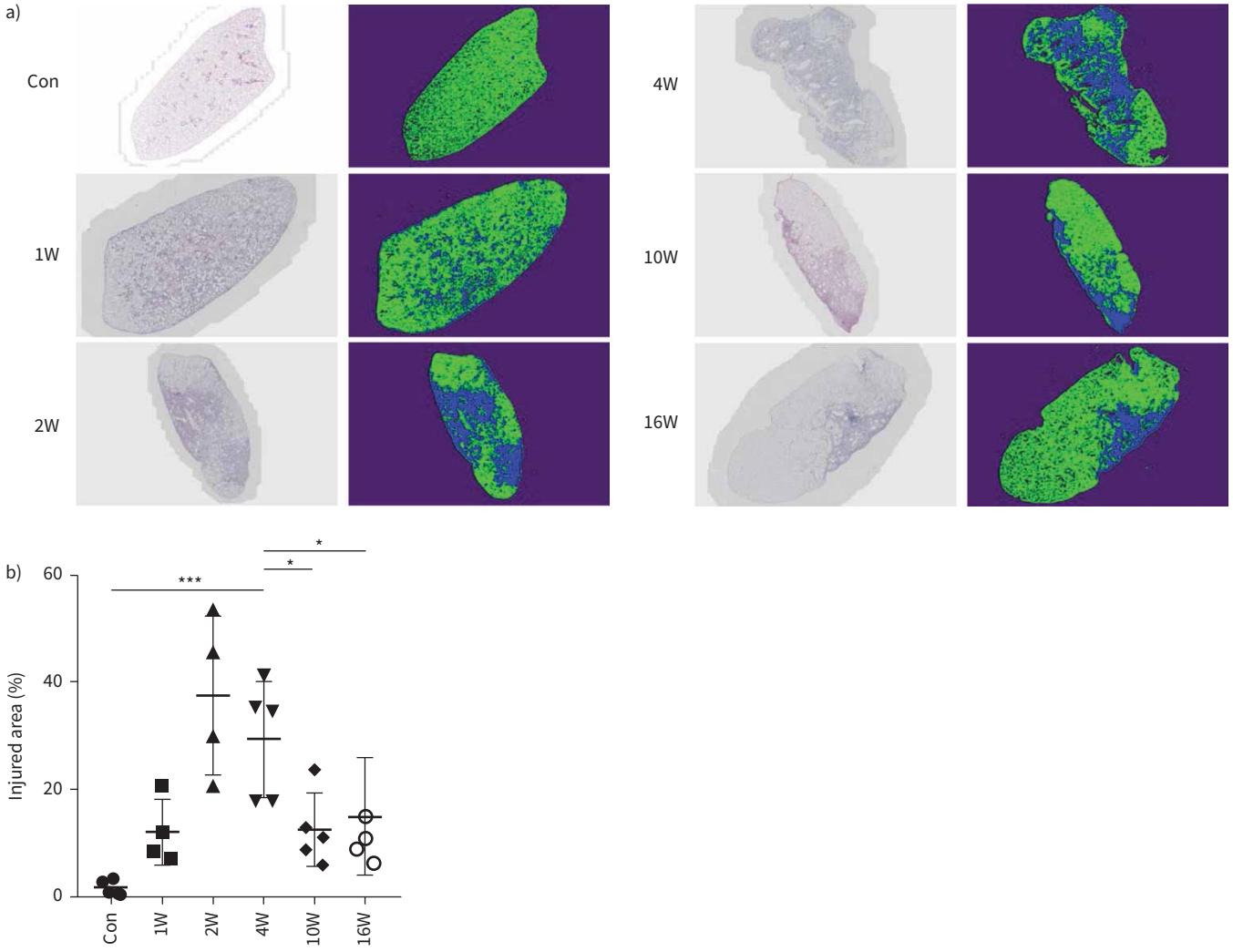

FIGURE 3 Histological assessment of lung tissues. a) Representative haematoxylin/eosin (HE)-stained whole-slide images (left) and their AI-processed results (right) using Orbit Image Analysis software. b) Calculation of the percentage of injured areas on HE-stained whole-slide images. Data are expressed as mean±SD, n=4. *: p<0.05; ***: p<0.001. Con: control; W: weeks.

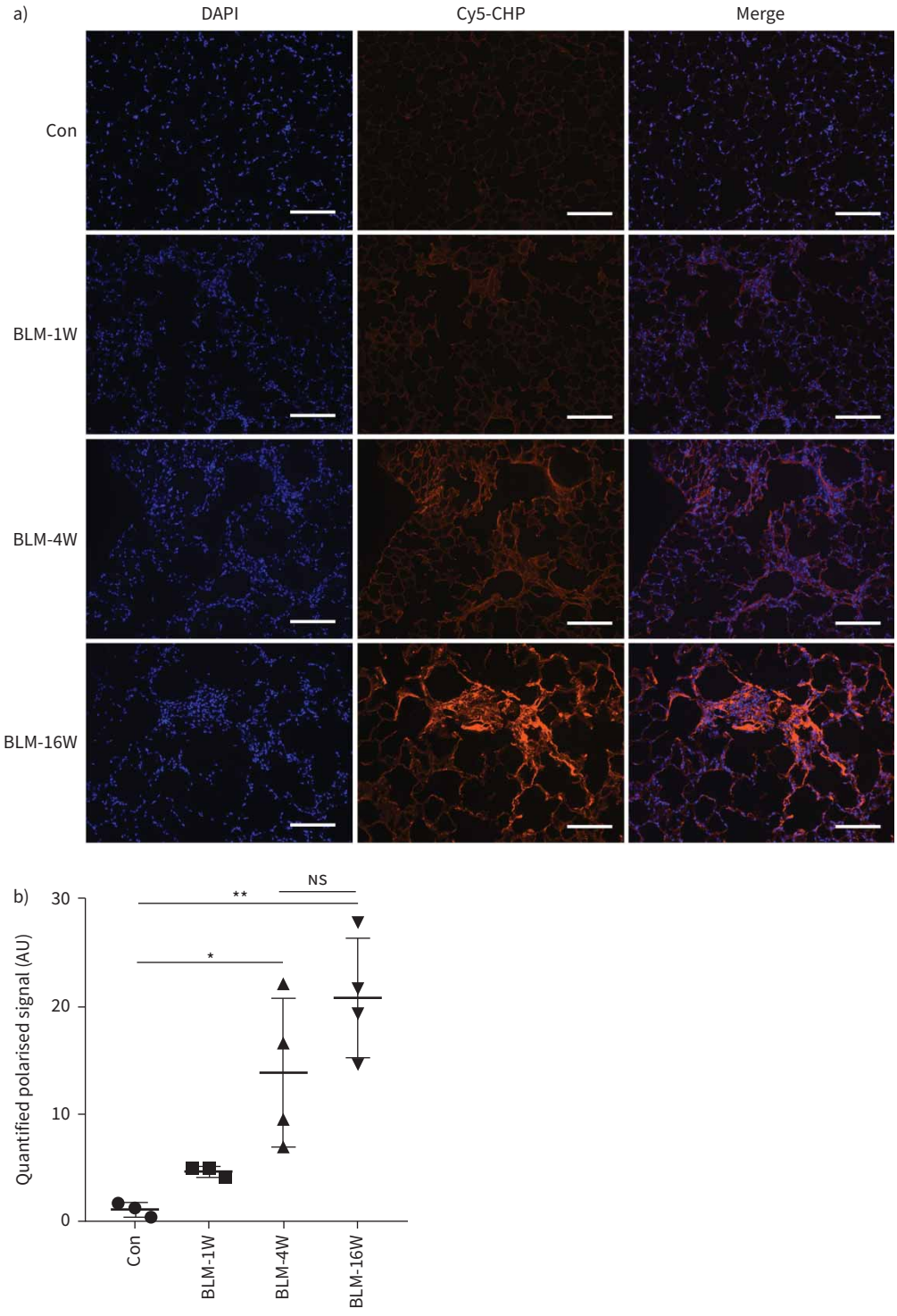

FIGURE 4 Histological detection of degraded collagens. a) Representative fluorescence micrographs of fibrotic lung areas obtained from mice treated with bleomycin for varying time periods *versus* control mice treated with saline, and stained with fluorescently labelled collagen hybridisation peptide (Cy5-CHP) and 4′,6-diamidino-2-phenylindole (DAPI). Selected micrographs are representative of images collected from each group. Scale bar: 200 μm. b) Quantified polarised signals (arbitrary units (AU)) showing the time course of Cy5-CHP signal levels. Data are expressed as mean±SD, n=3–6. *: p<0.05; **: p<0.01; NS: nonsignificant. Con: control; W: weeks.

In vivo *micro-CT analysis of lung structure and aeration*

To further validate the *in vitro* tissue data as well as to reduce animal-to-animal variability, the *in vivo* changes in lung structure or function were dynamically monitored by micro-CT imaging, which can provide longitudinal information on the same individual animal [6]. Representative lung transverse micro-CT sections from week 1 to week 16 after bleomycin treatment are shown in figure 5. It was demonstrated that the areas of lung consolidation reached a maximum level at week 4 and then gradually dwindled, hinting at a recovery course during the later stages of fibrosis.

To more subtly segment out those lung regions with partial or complete loss of aeration, a novel algorithm established by a recent study was also introduced into the present study, which accomplished the discrimination of poorly aerated and nonaerated regions with Hounsfield Unit thresholds ranging from −434 to −121 HU and −120 to 121 HU, respectively [23]. As indicated in figure 6a, the three types of regions with different conditions of aeration in fibrotic mice matched well with the visible structural alterations on transverse CT sections, suggesting the reliability of this method. Further lung volumetric analysis showed that the proportions of both poorly aerated and nonaerated regions were significantly increased before week 4, and then pronouncedly decreased between week 10 and week 16, whereas those of normally aerated areas exhibited the opposite trend (figure 6b). This result can be additionally validated by statistically measuring the corresponding values of multiple animals (figure 6c). Collectively, the *in vivo* data imply that bleomycin-triggered lung fibrosis was apt to spontaneously resolve.

Immunohistochemical assay of hydroxyproline-containing molecules

Because the hydroxyproline biochemical assay in tissues was conducted on their completely hydrolysed products, this method can in theory detect all forms of hydroxyproline-containing substances within tissues. Thus, we infer that the unchanged content of hydroxyproline under conditions of collagen degradation might be a result of incomplete removal of the substances from the tissue. To confirm this hypothesis, mouse lung tissues were subjected to immunohistochemical staining with specific antibody against hydroxyproline so as to observe its localisation. The lung interstitium in control mice was nearly negative for hydroxyproline, whereas those areas in the treated group at week 4 exhibited a wide distribution and moderate increase of hydroxyproline accumulation. In sharp contrast, at 10 or 16 weeks, the positive areas for hydroxyproline, albeit displaying a much more compact range, had dramatically enhanced intensity compared with those at week 4 (figure 7a). Notably, there occurred groups of cells with extremely strong intracellular immunostaining of hydroxyproline at both 10 and 16 weeks (figure 7a, arrows), while hydroxyproline-positive molecules appeared to be predominantly located within extracellular regions at 4 weeks. The total intensities of immunostaining signals for hydroxyproline were calculated to have no significant difference between week 4 and week 16 (figure 7b), which agrees perfectly with the data from the biochemical method. This first application of hydroxyproline-specific immunohistochemistry in lung fibrosis evaluation clearly indicated that hydroxyproline-rich collagen

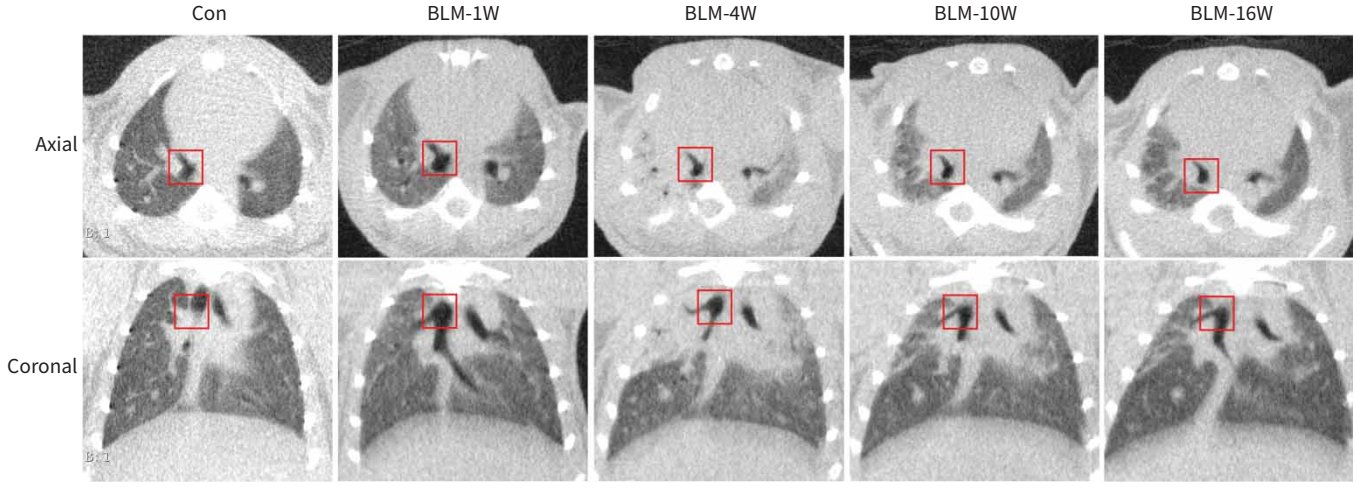

FIGURE 5 Micro-computed tomography (CT) images of the lungs. Axial (top row) and corresponding coronal (bottom row) images were acquired at different time-points after bleomycin (BLM) administration at a dose of 2.0 mg·kg^{-1}. At each time-point, the bifurcation of the right bronchus in mice was marked with a red square in order to ensure that the region was selected at the same position in all images. Con: control; W: weeks.

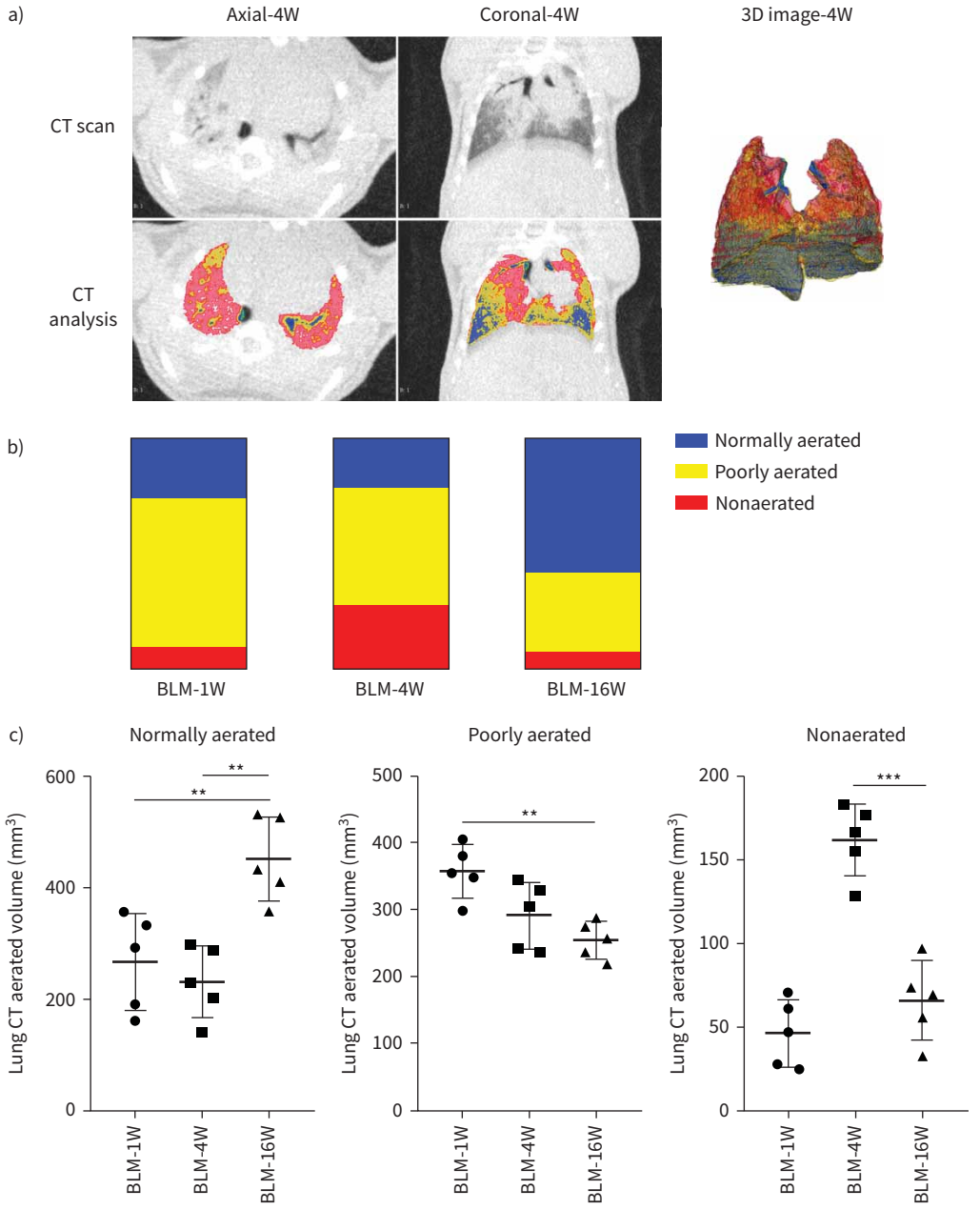

FIGURE 6 Quantitative computed tomography (CT) volumetric evaluation of lung aeration. a) Representative colour map analyses of lung CT images from bleomycin (BLM)-treated mice at week 4. Blue: normally aerated region; yellow: poorly aerated region; red: nonaerated region. b) Dynamic percentages of lung CT aerated volume in representative mice at the indicated time-points after BLM injury. c) Statistical analysis of lung CT aerated volume. Data are expressed as mean±SD, n=6. **: p<0.01; ***: p<0.001. 3D: three-dimensional; Con: control; W: weeks.

fragments could not be completely removed and catabolised even after long-term evolution of fibrosis (figure 8).

Discussion

To the best of our knowledge, this represents the most thorough and deep description of the bleomycin-induced pulmonary fibrosis process to date. In addition to traditional methods, several of the latest improved technologies for fibrosis assessment were also deliberately introduced and utilised, such as AI analysis of whole-slide images, CT-based quantification of lung aeration as well as determination of the

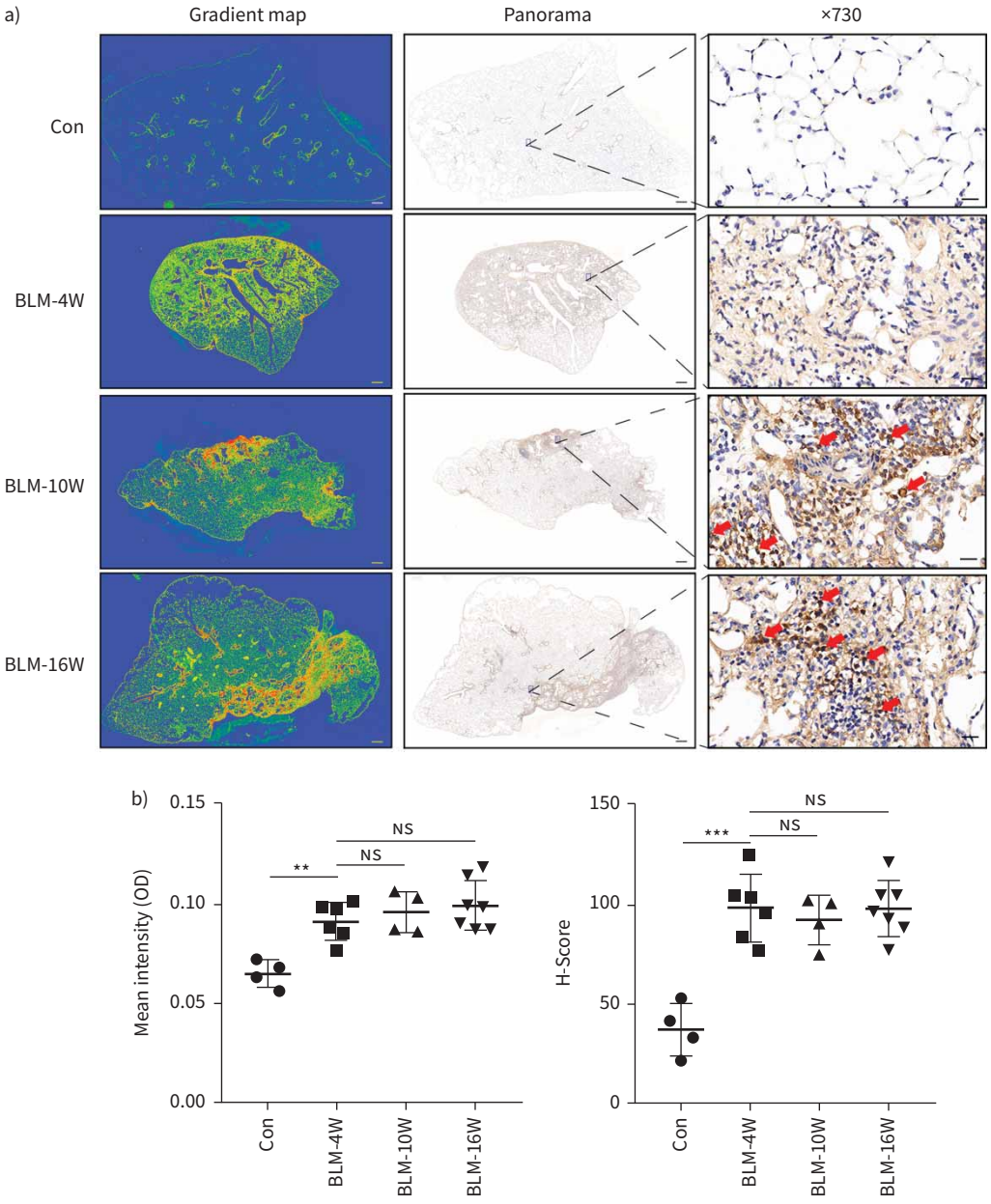

FIGURE 7 Immunohistochemical analysis of hydroxyproline content. a) Immunohistochemical stained panorama images (middle) for hydroxyproline and their respective gradient maps (left) of the indicated lung tissues. Scale bar: 500 μm. The right column indicates high power fields of positive staining areas. Scale bar: 20 μm. Arrows show cells with extremely strong intracellular immunostaining of hydroxyproline. b) The mean intensity (optical density (OD)) of immunostaining signals as well as the H-Score for hydroxyproline were calculated. Data are expressed as mean±SD, n=4–6. **: p<0.01; ***: p<0.001; NS: nonsignificant. Con: control; W: weeks.

unique triple-helical structure of collagen by CHP staining. Except for the biochemical assay of hydroxyproline content, most of the data from this study agree well with the popular conception that mouse lung fibrosis can spontaneously resolve. This odd inconsistency was finally reconciled by our application of immunohistochemistry to detect the distribution of hydroxyproline-containing molecules within fibrotic lung tissues.

Here, three different lines of evidence were presented to address a shift in the balance from collagen synthesis to degradation during the whole process of experimental fibrosis. 1) The expression of type I

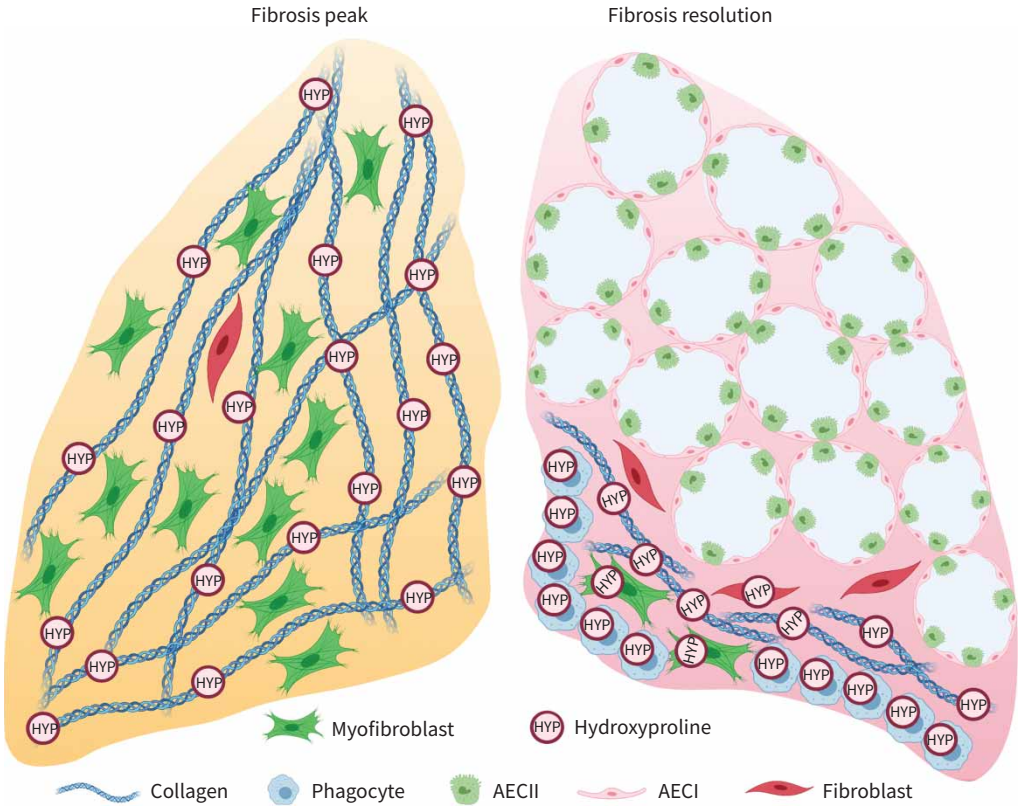

FIGURE 8 Schematic hypothesis of the constant content of hydroxyproline from fibrosis peak to valley periods. During the lung fibrosis peak, hydroxyproline-rich collagen fragments are largely deposited within the lung interstitium. Upon resolution of bleomycin-induced pulmonary fibrosis, collagen fibres might undergo enzymatic digestion and then be localised within a narrow area or even absorbed into the intracellular compartment. However, these hydroxyproline-containing substances may not be completely removed and catabolised, leading to the constant content of total hydroxyproline. AECI: alveolar epithelial cell type I; AECII: alveolar epithelial cell type II.

collagen, at the level of both transcription and translation, was dramatically decreased after a transient rise during the first 4 weeks. 2) Sirius red staining, considered to be specifically suitable for the evaluation of very small fibrotic lesions due to its high sensitivity [30], further confirmed the latter decline in new collagen proteins. 3) CHP staining of unfolded collagen chains directly validated the advent of collagen degradation after the fibrosis peak. However, our biochemical determination of hydroxyproline produced contradictory data, showing that the amount of total lung hydroxyproline reached a peak at 4 weeks after bleomycin injury and maintained a steady high level thereafter until the end of the experiments (16 weeks). The exceptional hydroxyproline data prompts us to first reconsider the potential influence from methodologies. Hydroxyproline can be quantified by high-performance liquid chromatography (HPLC), whereas the most widely used method is a colorimetric assay based on the reaction of oxidised hydroxyproline with *p*-dimethylaminobenzaldehyde [31]. By carefully searching the published literature for detailed information regarding hydroxyproline content in the mouse lung fibrosis model, we found two articles had reported similar results to ours, with one using HPLC [15] and the other one utilising the colorimetric assay [14]. Because these two previous independent studies did not investigate the exact status of native collagens, it remains unclear whether the nonequivalence of hydroxyproline content with native collagen quantity in the present study could be similarly observed. Whatever the conclusion, at least the phenomenon that bleomycin-induced augmentation of lung hydroxyproline in mice can sustain for a long duration has been demonstrated elsewhere [14, 15].

Collagen degradation occurs through both extracellular and intracellular pathways. The extracellular pathway involves cleavage of collagen fibrils by proteolytic enzymes, while the intracellular pathway involves binding and uptake of collagen fragments by fibroblasts or macrophages for lysosomal degradation [32]. In theory, biochemical determination of hydroxyproline is supposed to detect all forms of

hydroxyproline-containing substances, including native collagens, collagen fragments and free hydroxyproline. Therefore, elevated lung hydroxyproline content after injury, in addition to representing an increase in collagen production, could also mean a defect in the overall turnover of collagens [33]. Several pathways have been identified to internalise collagen fragments and consequently allow cells to clear and recycle matrix components [33–35]. Interestingly, compared with controls, mice deficient in those receptors responsible for collagen internalisation exhibit an increased total lung hydroxyproline content 4 weeks after bleomycin injury without alterations in inflammation or rates of collagen synthesis [33, 35]. Nevertheless, we did not find any significant changes in the expression levels of these genes between groups at weeks 4 and 16 (data not shown), implying that the process of collagen internalisation might function properly during this period. This speculation can be strengthened by the fact that hydroxyproline-rich molecules mostly reside within intracellular compartments of the cell at 10 or 16 weeks, a phenomenon which is completely absent at 4 weeks. According to the evidence, it is highly likely that the maintenance of an extraordinarily high level of hydroxyproline at the resolution phase of lung fibrosis might be caused by the incomplete clearance of collagen degradation products from the intracellular space (figure 8). Future studies need to focus on clarifying the detailed mechanisms underlying collagen turnover during the time window of lung fibrosis resolution.

In mammalian cells, there are a variety of types of protein modification at the post-translational level, such as phosphorylation, ubiquitination as well as hydroxylation. These modified amino groups can be immunoblotted with corresponding antibodies in combination with immunoprecipitation manipulation. As for anti-hydroxyproline antibodies, these have mostly been exploited to detect the events of proline hydroxylation of intracellular signal transducers [36, 37]. In the field of organ fibrosis, the biochemical assay of hydroxyproline has long been used as the "gold standard" for collagen content evaluation. Therefore, the current study represents the first to introduce the immunoassay of hydroxyproline to the study of fibrosis.

Even though our data and explanation seem reasonable, one point that could not be neglected is that the hydroxyproline content in those studies claiming the resolving nature of the bleomycin model trended downwards after the fibrosis peak [28, 38, 39], which is totally opposed to our current data. Although it remains unclear whether this discrepancy is associated with the source of bleomycin or animal species, we at least provide a possibility that the deposited collagens in the mouse lung fibrosis model might have the chance to be incompletely cleared under some circumstances. In addition, we also provide a powerful and easy-to-use technique to explore the destination of collagen degradation products in fibrotic lung tissues. This is propitious to reconcile the debate regarding the fibrosis recovery issue that is currently highly dependent on the biochemical assay of hydroxyproline.

Although CT scanning can report dynamic structural alterations caused by fibrotic lesions, and thus provide longitudinal and localisation information, lung CT imaging of small animals remains a challenge due to its relatively low resolution. CT can be calibrated using a reference values of air (−1000 HU), pure water (0 HU) and dense bone (+1000 HU). Two recent studies have tried to use the Hounsfield Unit value to subdivide the ventilated areas of fibrotic lesions in mice. Although Ruscitti *et al*. [40] defined poorly aerated areas in the range of −500 to −100 HU, they did not distinguish nonaerated regions that usually have a value higher than −100 HU. On the basis of analysing a large number of lung CT images of pulmonary fibrosis mice, another study proposed a new stratification standard for lung ventilation, which classified the poorly aerated and nonaerated regions as −434 to −121 HU and −120 to 121 HU, respectively [23]. We applied this novel algorithm to the current study and found that the lung ventilation function tended to spontaneously recover from 4 weeks after bleomycin, backing the self-limiting nature of this murine model reported by others [12, 28, 41]. To the best of our knowledge, ours is the first study to calculate the three-dimensional volume of lung lesions with different aeration conditions during sustained progression of experimental lung fibrosis and this will definitely act as a more reliable functional readout for future drug efficacy evaluation.

Regarding the multiple methodologies for fibrosis quantitation, we still believe that the biochemical assay of hydroxyproline content is the most objective and accurate method if collagen matrix synthesis dominates over destruction. However, in some cases, such as when studying the long duration of fibrosis or evaluating the efficacy of therapeutic agents that are potentially involved in collagen degradation, immunohistochemistry of hydroxyproline as well as CHP staining of denatured collagen are recommended in the first place to confirm whether intensive collagen degradation occurs.

In summary, our results showed that, at later stages of fibrosis, alterations in hydroxyproline content that are long considered as a "gold standard" for lung fibrosis assessment did not coincide with the changes of

other evaluation parameters, including histological staining, gene expression as well as lung aeration. This strikingly exceptional result was confirmed to be associated with the incomplete removal of degraded collagen fragments, as demonstrated by immunostaining of hydroxyproline. Hence, the data from the current study not only offer respiratory researchers a new perspective towards the resolution nature of the mouse pulmonary fibrosis process, but also remind them to be cautious when using the conventional hydroxyproline assay to reflect the amount of collagens.

Author contributions: Jin Su and Nanshan Zhong conceived the project and designed the experiments. Jin Su and Ruijuan Guan wrote the manuscript. Penghui Yang, Yang Li, Yunxin Lai and Jiangtian Yu edited the manuscript. Shengren Song, Zhenli Fu, Jie Zhao, Hang Yin and Gencheng Gong performed the experiments. Shengren Song, Zhenli Fu, Jie Zhao, Ying He, Simin Zhao, Xiaomin Peng and Yumei Luo conducted the data analysis. All authors have read and approved the final manuscript.

Conflict of interest: None declared.

Support statement: This work was supported by grants from the National Natural Science Foundation of China (31671472 and 81800072), the China Postdoctoral Science Foundation (2020T130027ZX), Guangdong Key Research and Development Project (2020B1111330001), and the COVID-19 Emerging Prevention Products, Research Special Fund of Zhuhai City (ZH22036302200024PWC). Funding information for this article has been deposited with the Crossref Funder Registry.

References

1 Martinez FJ, Collard HR, Pardo A, *et al.* Idiopathic pulmonary fibrosis. *Nat Rev Dis Primers* 2017; 3: 17074.
2 Raghu G. Epidemiology, survival, incidence and prevalence of idiopathic pulmonary fibrosis in the USA and Canada. *Eur Respir J* 2017; 49: 1602384.
3 Kolb P, Upagupta C, Vierhout M, *et al.* The importance of interventional timing in the bleomycin model of pulmonary fibrosis. *Eur Respir J* 2020; 55: 1901105.
4 Cruwys S, Hein P, Humphries B, *et al.* Drug discovery and development in idiopathic pulmonary fibrosis: challenges and opportunities. *Drug Discov Today* 2020; 25: 2277–2283.
5 Spagnolo P, Maher TM. Clinical trial research in focus: why do so many clinical trials fail in IPF? *Lancet Respir Med* 2017; 5: 372–374.
6 Jenkins RG, Moore BB, Chambers RC, *et al.* An Official American Thoracic Society Workshop Report: use of animal models for the preclinical assessment of potential therapies for pulmonary fibrosis. *Am J Respir Cell Mol Biol* 2017; 56: 667–679.
7 Tashiro J, Rubio GA, Limper AH, *et al.* Exploring animal models that resemble idiopathic pulmonary fibrosis. *Front Med* 2017; 4: 118.
8 Bonniaud P, Fabre A, Frossard N, *et al.* Optimising experimental research in respiratory diseases: an ERS statement. *Eur Respir J* 2018; 51: 1702133.
9 Liu T, De Los Santos FG, Phan SH. The bleomycin model of pulmonary fibrosis. *Methods Mol Biol* 2017; 1627: 27–42.
10 Moore BB, Hogaboam CM. Murine models of pulmonary fibrosis. *Am J Physiol Lung Cell Mol Physiol* 2008; 294: L152–L160.
11 Borzone G, Moreno R, Urrea R, *et al.* Bleomycin-induced chronic lung damage does not resemble human idiopathic pulmonary fibrosis. *Am J Respir Crit Care Med* 2001; 163: 1648–1653.
12 Lawson WE, Polosukhin VV, Stathopoulos GT, *et al.* Increased and prolonged pulmonary fibrosis in surfactant protein C-deficient mice following intratracheal bleomycin. *Am J Pathol* 2005; 167: 1267–1277.
13 Chung MP, Monick MM, Hamzeh NY, *et al.* Role of repeated lung injury and genetic background in bleomycin-induced fibrosis. *Am J Respir Cell Mol Biol* 2003; 29: 375–380.
14 Limjunyawong N, Mitzner W, Horton MR. A mouse model of chronic idiopathic pulmonary fibrosis. *Physiol Rep* 2014; 2: e00249.
15 Scotton CJ, Hayes B, Alexander R, *et al. Ex vivo* micro-computed tomography analysis of bleomycin-induced lung fibrosis for preclinical drug evaluation. *Eur Respir J* 2013; 42: 1633–1645.
16 Stritt M, Stalder AK, Vezzali E. Orbit Image Analysis: an open-source whole slide image analysis tool. *PLoS Comput Biol* 2020; 16: e1007313.
17 Seger S, Stritt M, Vezzali E, *et al.* A fully automated image analysis method to quantify lung fibrosis in the bleomycin-induced rat model. *PLoS One* 2018; 13: e0193057.
18 Cocconcelli E, Balestro E, Biondini D, *et al.* High-resolution computed tomography (HRCT) reflects disease progression in patients with idiopathic pulmonary fibrosis (IPF): relationship with lung pathology. *J Clin Med* 2019; 8: 399.

19 Ruscitti F, Ravanetti F, Essers J, *et al.* Longitudinal assessment of bleomycin-induced lung fibrosis by micro-CT correlates with histological evaluation in mice. *Multidiscip Respir Med* 2017; 12: 8.

20 Lee HJ, Goo JM, Kim NR, *et al.* Semiquantitative measurement of murine bleomycin-induced lung fibrosis in *in vivo* and postmortem conditions using microcomputed tomography: correlation with pathologic scores – initial results. *Invest Radiol* 2008; 43: 453–460.

21 Ruscitti F, Ravanetti F, Donofrio G, *et al.* A multimodal imaging approach based on micro-CT and fluorescence molecular tomography for longitudinal assessment of bleomycin-induced lung fibrosis in mice. *J Vis Exp* 2018; 134: 56443.

22 Zhou Y, Chen H, Ambalavanan N, *et al.* Noninvasive imaging of experimental lung fibrosis. *Am J Respir Cell Mol Biol* 2015; 53: 8–13.

23 Mecozzi L, Mambrini M, Ruscitti F, *et al.* In-vivo lung fibrosis staging in a bleomycin-mouse model: a new micro-CT guided densitometric approach. *Sci Rep* 2020; 10: 18735.

24 Bell RD, Rudmann C, Wood RW, *et al.* Longitudinal micro-CT as an outcome measure of interstitial lung disease in TNF-transgenic mice. *PLoS One* 2018; 13: e0190678.

25 Campa JS, McAnulty RJ, Laurent GJ. Application of high-pressure liquid chromatography to studies of collagen production by isolated cells in culture. *Anal Biochem* 1990; 186: 257–263.

26 Kliment CR, Englert JM, Crum LP, *et al.* A novel method for accurate collagen and biochemical assessment of pulmonary tissue utilizing one animal. *Int J Clin Exp Pathol* 2011; 4: 349–355.

27 Gharaee-Kermani M, Hatano K, Nozaki Y, *et al.* Gender-based differences in bleomycin-induced pulmonary fibrosis. *Am J Pathol* 2005; 166: 1593–1606.

28 Caporarello N, Meridew JA, Jones DL, *et al.* PGC1alpha repression in IPF fibroblasts drives a pathologic metabolic, secretory and fibrogenic state. *Thorax* 2019; 74: 749–760.

29 Hwang J, Huang Y, Burwell TJ, *et al. In situ* imaging of tissue remodeling with collagen hybridizing peptides. *ACS Nano* 2017; 11: 9825–9835.

30 Malkusch W, Rehn B, Bruch J. Advantages of Sirius Red staining for quantitative morphometric collagen measurements in lungs. *Exp Lung Res* 1995; 21: 67–77.

31 Hofman K, Hall B, Cleaver H, *et al.* High-throughput quantification of hydroxyproline for determination of collagen. *Anal Biochem* 2011; 417: 289–291.

32 McKleroy W, Lee TH, Atabai K. Always cleave up your mess: targeting collagen degradation to treat tissue fibrosis. *Am J Physiol Lung Cell Mol Physiol* 2013; 304: L709–L721.

33 Atabai K, Jame S, Azhar N, *et al.* Mfge8 diminishes the severity of tissue fibrosis in mice by binding and targeting collagen for uptake by macrophages. *J Clin Invest* 2009; 119: 3713–3722.

34 Lee W, Sodek J, McCulloch CA. Role of integrins in regulation of collagen phagocytosis by human fibroblasts. *J Cell Physiol* 1996; 168: 695–704.

35 Bundesmann MM, Wagner TE, Chow YH, *et al.* Role of urokinase plasminogen activator receptor-associated protein in mouse lung. *Am J Respir Cell Mol Biol* 2012; 46: 233–239.

36 Arquier N, Vigne P, Duplan E, *et al.* Analysis of the hypoxia-sensing pathway in *Drosophila melanogaster*. *Biochem J* 2006; 393: 471–480.

37 Luo W, Hu H, Chang R, *et al.* Pyruvate kinase M2 is a PHD3-stimulated coactivator for hypoxia-inducible factor 1. *Cell* 2011; 145: 732–744.

38 Hecker L, Logsdon NJ, Kurundkar D, *et al.* Reversal of persistent fibrosis in aging by targeting Nox4-Nrf2 redox imbalance. *Sci Transl Med* 2014; 6: 231ra47.

39 Cabrera S, Selman M, Lonzano-Bolanos A, *et al.* Gene expression profiles reveal molecular mechanisms involved in the progression and resolution of bleomycin-induced lung fibrosis. *Am J Physiol Lung Cell Mol Physiol* 2013; 304: L593–L601.

40 Ruscitti F, Ravanetti F, Bertani V, *et al.* Quantification of lung fibrosis in IPF-like mouse model and pharmacological response to treatment by micro-computed tomography. *Front Pharmacol* 2020; 11: 1117.

41 Glasser SW, Hagood JS, Wong S, *et al.* Mechanisms of lung fibrosis resolution. *Am J Pathol* 2016; 186: 1066–1077.